Effect of swift heavy ion irradiations in polycrystalline aluminum nitride

— Source link ↗

Jean-Christophe Nappé, Mourad Benabdesselam, Philippe Grosseau, Bernard Guilhot

Institutions: École Normale Supérieure, University of Nice Sophia Antipolis

Related papers:

- Afterglow in bulk AlN single crystals under β-irradiation

- Dynamics of changes in structural properties of AlN ceramics after Xe+22 ion irradiation

- A comparison of Ar ion implantation and swift heavy Xe ion irradiation effects on immiscible AlN/TiN multilayered nanostructures

- On the conflicting roles of ionizing radiation in ceramics

- Ion irradiation stability of multilayered AlN/TiN nanocomposites

Effect of swift heavy ion irradiations in polycrystalline aluminum nitride

Jean-Christophe Nappé, Mourad Benabdesselam, Philippe Grosseau, Bernard Guilhot

Effect of swift heavy ion irradiations in polycrystalline aluminum nitride

J.C. Nappé[a,*], M. Benabdesselam[b], Ph. Grosseau[a], B. Guilhot[c]

[a] École Nationale Supérieure des Mines, SPIN/PMMC, LPMG UMR CNRS 5148, 158 cours Fauriel, 42023 Saint-Étienne cedex 2, France

[b] Université de Nice - Sophia Antipolis, LPMC UMR CNRS 6622, Parc Valrose, 06108 Nice cedex 2, France

[c] École Nationale Supérieure des Mines, CIS, 158 cours Fauriel, 42023 Saint-Étienne cedex 2, France

ABSTRACT

Thanks to its high thermal conductivity, aluminum nitride may be a serious candidate as fuel coating for the Gas Fast Reactor. However, its behavior under irradiation is not entirely well understood. In order to catch a glimpse of this behavior, specimens were irradiated with swift heavy ions of different energies then characterised by both thermally stimulated luminescence and optical absorption spectrophotometry. With these techniques, the native defects, as well as those affected by irradiation, were identified: thus, by comparison to the virgin sample, no new defect detectable by these techniques is created by irradiations. Eventually, the fact that these techniques complement each other allowed to understand the effect of irradiation parameters on the defect concentration.

Keywords: AlN, irradiation, swift heavy ions, electronic interactions, thermoluminescence, optical absorption spectrophotometry

PACS: 77.84.Bw, 61.82.Ms, 61.80.Lj, 25.75.Ag, 34.50.Bw, 28.41.Bm, 78.60.Kn, 78.20.Ci

1. Introduction

Gas Fast Reactor (GFR) is one of the six new systems considered by Generation IV International Forum (GIF): it is designed to work under helium-pressure and high-temperature (1100-1300 K). These working conditions led to the selection of non-oxide refractory ceramics as fuel coating; the remarkable thermo-mechanical properties of carbides and nitrides make them great candidates for this application. However, their behavior under irradiation has to be studied in more details.

Among the studied materials, aluminum nitride is distinguished by its high thermal conductivity which should ensure the heat transfer between the coolant and the fuel. Actually, the values obtained for commercial aluminum nitride generally range between 160 and 200 W m^{-1} K^{-1} [1-4] with the highest value of 320 W m^{-1} K^{-1} measured on a single crystal [5].

---

* Corresponding author. Tel.: +33 477 420 213; fax: +33 477 499 694.
  E-mail: jc.nappe@yahoo.fr.

The main drawback for the use of aluminum nitride in nuclear facilities is its ability to generate a radioactive long-lived isotope ^{14}C by transmutation of ^{14}N [6]. Nevertheless, this drawback can be reduced by the use of isotope tailored material, in which ^{15}N replaces ^{14}N [7].

The behavior of aluminum nitride ceramics is also studied in the framework of fusion reactors, in which this material, thanks to its high electrical resistivity (> 10^{12} Ω m at 300 K [8]), could be used as electric insulator for toroidal current break, neutral beam injectors, and superconducting magnets. Thus, many works have been carried out to understand the behavior of aluminum nitride under neutron irradiation, especially by Yano *et al.* [7,9-17]. However, as far as we know, no study has been performed concerning the characterization of defects induced by irradiation.

Thus, the aim of this study is to characterize the evolution of native defects of aluminum nitride as a result of swift heavy ion irradiations, using thermally stimulated luminescence and optical absorption spectrophotometry.

2. Material and methods

2.1. Sample preparation and irradiation

The studied material was obtained by sintering of AlN powders with Y_2O_3 (sintering aid: 3 mol%) at 2123 K in nitrogen atmosphere during 3 h. This polycrystalline aluminum nitride consists of 8 µm grains with 0.89 % of oxygen. Its thermal conductivity was measured between 198 and 214 W m^{-1} K^{-1}. Preparation of the samples before irradiation was already described elsewhere [18]. Briefly, they were polished with diamond suspensions down to 1 µm, and then subsequently irradiated with different swift heavy ions (SHI). This kind of irradiation aims to simulate the interactions of fission products without the drawback of neutrons activating the specimens. Thus, the specimens can be manipulated just after irradiations without any particular precautions.

SHI were provided by GANIL facilities (Caen, France). In order to know the effect of electronic stopping power, samples were irradiated with different ion-energy couples. Table 1 shows the effect of three ion irradiations in AlN, to wit the average projected range (Rp), both the electronic (Se) and the nuclear (Sn) stopping powers. All these data were obtained with SRIM-2008 code [19]. In addition, this table contains the experimentally reached fluences and the irradiation temperatures.

Table 1: Summary of irradiation conditions; RT stands for room temperature.

Ion irradiation	Rp (µm)	Se (keV nm^{-1})	Sn (keV nm^{-1})	Fluences (cm^{-2})	Temperatures
74 MeV Kr	9.7	13.1	0.054	10^{12}, 10^{13}, 10^{14}, 10^{15}	RT & 773 K
92 MeV Xe	9.4	17.7	0.132	10^{12}, 10^{13}, 10^{14}, 10^{15}	RT
930 MeV Xe	46.2	21.8	0.018	10^{11}, 10^{12}, 10^{13}, 4.5×10^{13}	RT & 773 K

The fluences reached for 930 MeV Xe irradiations are lower than those reached with the two other irradiations. This is due to the highest energy, which may heat the samples during irradiation. Thus, in order not to heat the samples, the flux used for this irradiation was lower than for the two others. The required duration for equivalent fluences were hence much higher.

2.2. Thermally stimulated luminescence measurements

Principle of thermally stimulated luminescence (TSL) may be found elsewhere [20,21]. For TSL measurements, specimens were excited at room temperature (RT) during five minutes by a deuterium UV-lamp (50 W) covering the 200-400 nm spectral range.

Two minutes after excitation, TSL readout was achieved by linear heating of the excited sample from RT to 673 K at a rate of 1 K s^{-1}. TSL intensity was recorded by means of a photomultiplier (Philips 2018 B) covering the 200-600 nm range. For spectral analyzis of TSL emission, spectra were caught by an optical multi-channel analyzer (Princeton Instruments) covering the 300-800 nm range.

2.3. Optical absorption measurements

Optical absorption spectrophotometry (OAS) was performed at room temperature using a Varian Carry 500 spectrophotometer equipped with a diffuse reflection sphere. The spectra were recorded on the 250-800 nm wavelength range with a scan rate of 600 nm min^{-1}. The absorption reference was made of polytetrafluoroethylene (PTFE). For all the samples, optical absorption was measured before and after ion irradiation in the same experimental conditions. The absorption bands affected by irradiation have been characterized by the difference curve, which is obtained by subtracting the absorption spectrum of the virgin sample from the spectrum of the same sample after ion irradiation.

3. Results

3.1. Thermally Stimulated Luminescence

Typical evolution of TSL glow curves as a function of fluence is shown in Figure 1. The TSL signal of the AlN sample before irradiation consists of one broad and structureless glow curve peaking at approximately 400 K. This broad peak is due to the presence of oxygen in the nitrogen sublattice. More precisely, it attests the presence of trapping centers (TC), certainly oxygen in substitution of nitrogen O_N and/or bivalent $2O_N$ centers [20,22,23]. Whatever the ion-energy couple or the irradiation temperature are, the TSL intensity decreases with increasing fluence. Moreover, neither shift of the main peak, nor presence of new TSL peaks induced by irradiation were observed.
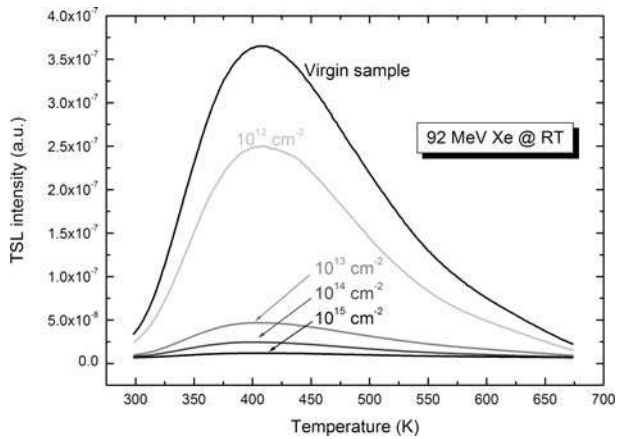
3

Figure 1: TSL glow curves of polycrystalline AlN sample as a function of 92 MeV Xe ion fluence.

In order to compare the TSL signal for each irradiation, we calculated the area under each glow curve; Figure 2 shows the variation of TSL area as a function of fluence for each irradiation. In this Figure, we can note three different trends. First, for 74 MeV Kr and 92 MeV Xe irradiations at RT, TSL area quickly decreases up to 10^{13} cm^{-2} then tends to stabilize. Second, for irradiation at 773 K with 74 MeV Kr we can note a slight decrease up to 10^{13} cm^{-2} followed by a sharp decline occuring between 10^{13} and 10^{14} cm^{-2}, then finally a stabilization of the signal. Third, whatever the temperature of 930 MeV Xe irradiation is, TSL area decreases more swiftly than for other irradiations up to stabilization. These trends suggest that the degradation process revealed by TSL is the same for different irradiations but of similar energies.
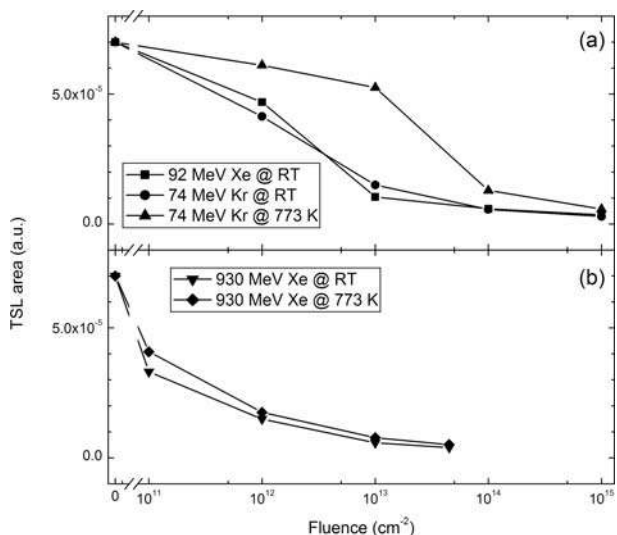

Figure 2: TSL area under glow curve as a function of ion fluence for (a) low energy irradiations, and (b) high energy irradiations; lines are only to guide the eye.

4

Figure 3 shows the typical evolution of TSL emission spectra of the main peak (400 K) as a function of fluence; position of the bands was determined by Gaussian decomposition (not shown here). The spectrum of the virgin sample shows the main recombination centers (RC) in AlN already identified by Benabdesselam *et al.* [21]. First, the main broad band centered at around 3.2 eV is the convolution of the emission of probably three RC, which are more easily noticeable for the highest fluences (see inset): the emissions at 3.17 ± 0.01 eV and 2.67 ± 0.17 eV have been respectively attributed to complex centers V_{Al}-O_N-3N and V_{Al}-$2O_N$-2N while the one at 3.60 ± 0.04 eV may be associated to transitions from V_{Al} to O_N [22]. Concerning the low bands appearing at lower energies, they might be linked to some impurities: the emission at 2.04 ± 0.05 eV is attributed to the presence of Mn^{4+} in substitution of Al^{3+} (Mn_{Al}) [21] whereas that centered at 1.79 ± 0.03 eV has been reported by Martin *et al.* as being due to the presence of Cr^{3+} in substitution of Al^{3+} (Cr_{Al}) [24]. Inductively coupled plasma (ICP) analyzis confirmed the presence of both impurities in our samples, at concentrations of 1.9 ± 0.1 and 2.0 ± 0.1 ppm respectively.
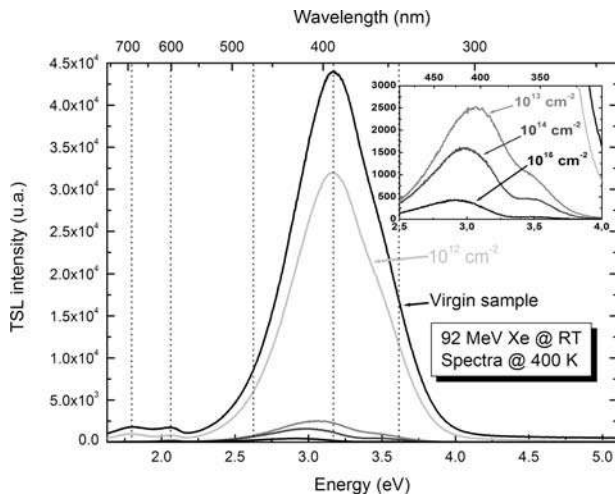

Figure 3: Spectral distribution of the main TSL peak (400 K) as a function of 92 MeV Xe ion fluence in polycrystalline AlN samples; the inset is a zoom of the main emission band for the highest fluences.

After irradiation, it is interesting to remark that no new RC is created: as shown for the glow curves, the intensity of the spectra decreases with the fluence, whatever the irradiation is.

3.2. Optical absorption spectrophotometry

Figure 4a shows the optical absorption spectrum of AlN before irradiation. It presents several absorption bands in the 250-800 nm range. In this Figure, one can see the spectrum of the sample irradiated at RT with 92 MeV Xe to 10^{15} cm^{-2}; as explained in section 2.3., the induced absorption was obtained by subtracting the absorption spectrum of a virgin sample from that of the same sample after ion irradiation.
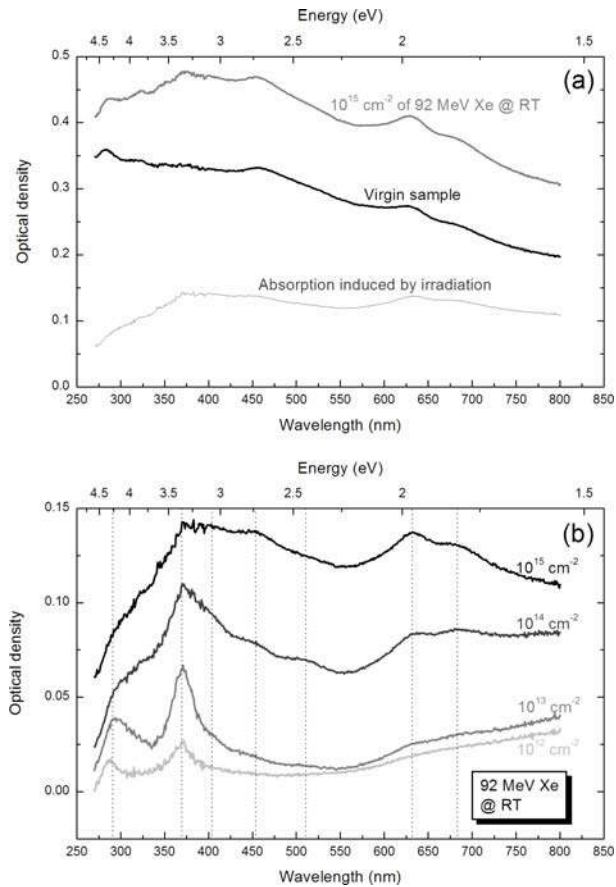
Figure 4: Optical absorption of polycristalline AlN in the 250-800 nm wavelength range: (a) comparison between the virgin sample and the same sample irradiated at room temperature with 92 MeV Xe to 10^{15} cm^{-2}, and (b) optical absorption bands induced by 92 MeV Xe irradiation.

Through the 92 MeV Xe irradiations, Figure 4b shows the typical evolution of the absorption induced by irradiation as a function of fluence. In this Figure, one can see an increase of the absorption with the fluence all over the studied range. After irradiation, the optical density of 7 bands increases more particularly; the energy of these bands (Table 2) was determined after Gaussian decomposition of the obtained spectra (not shown here). Each of these 7 bands was ever on the absorption spectrum of the virgin sample: irradiations do not induce any new absorbing defect in the 250-800 nm range.

Table 2: Identification of absorption bands affected by 92 MeV Xe irradiation in polycristalline AlN sample; F centers are defects based on anionic vacancies.

λ (nm)	E (eV)	Related defect	References
678 ± 7	1.83 ± 0.02	Cr^{3+} (zero-phonon)	[25-29]
630 ± 6	1.97 ± 0.02	Fe_{Al}	[30]
511 ± 6	2.43 ± 0.03	?	
455 ± 9	2.73 ± 0.05	V_N or Al_i or F_2^{2+}	[31-36]
406 ± 8	3.06 ± 0.06	V_{Al} or Cr_{Al}	[37,38]
370 ± 6	3.35 ± 0.05	F_2^+	[39]
290 ± 8	4.28 ± 0.12	O related center (F_2?) or Al_i	[36,40-42]

In the literature, few information are available concerning the identification of absorbing defects in AlN. The data presented in Table 2 has been performed using those from other materials, in particular from alumina. Indeed, according to the high chemical affinity of oxygen towards aluminum, it is likely that a thin layer of alumina is present on the surface of AlN samples. Finally, as for the impurities of both manganese and chromium observed in the TSL emission spectra, the presence of iron in AlN samples (Table 2) was clearly identified by ICP, at a ratio of 330 ± 20 ppm.

4. Discussion

The estimation of the concentration of each absorbing defect (AD) is complicated. However, for each irradiation parameter, we observed that when an absorption band increases, all the other bands do likewise, even if not with the same rate (Figure 4b); this observation was also right for decrease of the optical density of the irradiated sample compared with that of the virgin one. That is why, in order to understand the effects of SHI in AlN material, we decided to follow the variation of the overall absorption of each sample as a function of irradiation parameters by calculating, for each performed irradiation, the average of the optical density induced by irradiation; this global absorption was called average optical absorption induced by irradiation (Figure 5).
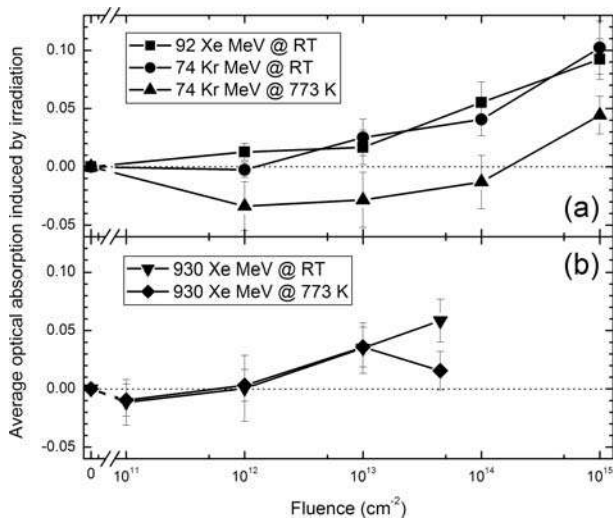
Figure 5: Average optical absorption induced by (a) low energy irradiations, and (b) high energy irradiations within the 250-800 nm wavelength range; lines are only to guide the eye.

Thus, whatever the irradiation carried out at RT is, the induced absorption remains constant and almost null up to 10^{12} cm^{-2}, and then increases. For irradiations performed at 773 K with 930 MeV Xe ions, the variation is similar to that at RT except for highest fluence of 4.5×10^{13} cm^{-2} for which the induced absorption decreases slightly at 773 K while it increases for RT. This behavior could be explained by an annealing of the defects created by irradiation from a critical fluence ϕ_c ranging between 10^{13} and 4.5×10^{13} cm^{-2} at 773 K. Thus, above ϕ_c the defects would be annealed, inducing a decrease of the overall concentration of defects. Finally, for the 74 MeV Kr irradiation at 773K, we observe a sharp drop in absorption compared to the virgin sample. This drop is followed by the same increase with the fluence as obtained for irradiation at RT: the average induced absorption hence reachs a comparable value to that before irradiation for 10^{14} cm^{-2} fluence, and becomes higher for 10^{15} cm^{-2}. Thus, if the electronic stopping power Se decreases (13.1 keV nm^{-1} for 74 MeV Kr and 21.8 keV nm^{-1} for 930 MeV Xe, see Table 1), the critical fluence of annealing ϕ_c decreases, being lower than 10^{12} cm^{-2} for irradiation at 773 K with 74 MeV Kr. Moreover, the evolution of this average induced absorption reflects a balance between annealing by irradiation temperature and creation of defects by irradiation itself, which inclines toward the creation only for high fluences.

Thanks to OAS, we know that irradiations create defects that absorb the UV-visible radiations, and therefore some of the TSL emissions mainly located in this range. To better understand the irradiation effects due to SHI, we now compare the results obtained by both techniques.

First, by considering the annealing at 773 K of the absorbing defects induced by 74 MeV Kr ion irradiation (Figure 5a), one would expect an increase of the TSL signal for low 74 MeV Kr fluences, above the signal of the virgin sample.

8

However, according to Figure 2a, the TSL signal also decreases for this irradiation. Therefore, this ion-energy couple (74 MeV Kr) seems to induce the decrease of TSL center concentration. Moreover, regarding the fact that there is no difference between the TSL signals related to 930 MeV Xe irradiations performed at RT and 773 K, we can consider that an increase of the irradiation temperature does not induce any increase of TSL center concentration, but only the annealing of AD. Therefore, the differences between the TSL curves of 74 MeV Kr ion irradiations would be only due to both the creation of AD at RT and their annealing at 773 K.

Second, for the same fluences and for irradiations performed at RT, TSL signal is nearly the same for both 74 MeV Kr and 92 MeV Xe irradiations, and then decreases in the case 930 MeV Xe irradiation. As for these irradiations the AD concentration is the same whatever the electronic stopping power is, this latter has not any effect on TSL center concentration up to a threshold Se_{th} above which this concentration strongly decreases; according to data reported in Table 1, this threshold would be between 17.7 and 21.8 keV nm^{-1}.

Eventually, when the fluence increases at RT, we noted that both the AD concentration increases in the same way whatever the Se is, and the TSL signal decreases as a function of Se. Therefore, the decrease of TSL signal as a function of the fluence cannot directly be attributed to the creation of AD. So we can conclude that when the fluence increases, the concentration of TSL centers decreases.

Thus, by comparing the TSL and OAS signals we now understand the effect of each irradiation parameter on the concentrations of both TSL centers and AD. But how to justify the fact that TSL center concentration decreases when either the electronic stopping power or the fluence increases? The first hypothesis is that, following the thermal spike model [43,44], electronic stopping power provides heat in the material through electron-phonon interactions. This heat could induce some annealing effect as ever remarked by Benyagoub *et al.* in silicon carbide [45]. Thus, the TSL center would be annealed, explaining the decrease of the TSL signal when increasing the fluence. Nevertheless, TSL centers observed in our specimens being due to the substitution of both Al and N atoms by impurities (oxygen, chromium, manganese, ...), their annealing appears to be difficult. Therefore, we rather think that electronic stopping power induces some modifications of these TSL centers. For instance, Mn^{4+} which is in substitution of Al^{3+} may be ejected from its site Mn_{Al} and becomes an intersticial Mn_i, or the complex centers V_{Al}-O_N-3N and V_{Al}-2O_N-2N may be dissociated by Se; these modifications may also be met with trapping centers such as oxygen in substitution of nitrogen. This hypothesis would explain the decrease of the concentration of TSL centers all the while creating other (absorbing) defects in the material. Whatever the hypothesis is, further characterisations would be necessary; for example, photoluminescence measurements would allow us to know the variation of the recombination center concentration as function of the irradiation parameters.

9

5. Conclusion

In this study, we first identified both trapping and recombination centers by thermally stimulated luminescence, but not all the absorbing defects are affected by SHI irradiation. A major result is that whatever the analytical technique is, no new defect was detected after these irradiations.

Second, thanks to the fact that TSL and OAS complement each other, we discriminated the effect of fluence, electronic stopping power, and temperature on the overall concentration of both TSL centers and AD. Thus, the higher the fluence, the lower the TSL center concentration, and the higher the AD concentration. Moreover, we defined an electronic stopping power threshold Se_{th}, which ranges between 17.7 and 21.8 keV nm^{-1}, above which the TSL center concentration strongly decreases. On the contrary, when $Se < Se_{th}$, the electronic stopping power has no effect on both TSL centers and AD concentrations. Concerning the temperature, we concluded that this parameter has no effect on TSL center concentration, whereas it induces the decrease of the AD concentration if the fluence is higher than a critical fluence ϕ_c which depends on ion-energy couple. This result is quite encouraging for application of aluminum nitride as a component of fuel for the GFR, which should operate at temperatures well above 773 K.

Eventually, we tried to know how the TSL signal decreases as a function of both electronic stopping power and fluence, and our hypothesis is that irradiations induce a change of the TSL centers, creating non-luminescent defects.

Acknowledgment

References

[1]   R. Couturier, D. Ducret, P. Merle, J. P. Disson, P. Joubert, Elaboration and characterization of a metal matrix composite: Al/AlN, J. Eur. Ceram. Soc. 17 (1997) 1861-1866.

[2]   F. Roulet, P. Tristant, J. Desmaison, R. Rezakhanlou, M. Ferrato, Corrosion behaviour of aluminium nitride in liquid aluminium: Influence of the microstructure, J. Eur. Ceram. Soc. 17 (1997) 1877-1883.

[3]   J. Jarrige, J.P. Lecompte, J. Mullot, G. Müller, Effect of oxygen on the thermal conductivity of aluminium nitride ceramics, J. Eur. Ceram. Soc. 17 (1997) 1891-1895.

[4]   A.V. Virkar, T.B. Jackson, R.A. Cutler, Thermodynamic and Kinetic Effects of Oxygen Removal on the Thermal Conductivity of Aluminum Nitride, J. Am. Ceram. Soc. 72 (1989) 2031-2042.

[5]   G.A. Slack, S.F. Bartram, Thermal expansion of some diamondlike crystals, J. Appl. Phys. 46 (1975) 89-98.

[6]   L.H. Rover, G.R. Hopkins, Nucl. Technol. 29 (1976) 274.

[7]   T. Yano, K. Inokuchi, M. Shikama, J. Ukai, S. Onose, T. Maruyama, Neutron irradiation effects on isotope tailored aluminum nitride ceramics by a fast reactor up to 2 × 1026 n/m2, J. Nucl. Mater. 329-333 (2004) 1471-1475.

[8]   Abdeslem Hafidi, Contribution à l'étude des propriétés thermiques de céramiques à base de nitrure d'aluminium, Thèse de doctorat, spécialité Sciences des Matériaux. Université de Limoges (1992).

[9]   T. Yano, T. Iseki, A HREM study of neutron-irradiation-induced dislocations in aluminum nitride, Philos. Mag. Lett. 62 (1990) 83-87.

[10]   T. Yano, H. Miyazaki, T. Iseki, Effect of isochronal annealing on thermal diffusivity of neutron-irradiated AlN, J. Nucl. Mater. 230 (1996) 74-77.

[11]   T. Yano, T. Iseki, High-resolution electron microscopy of neutron-irradiation-induced dislocations in SiC, Philos. Mag. A 62 (1990) 421-430.

[12]   T. Yano, M. Tezuka, H. Miyazaki, T. Iseki, Macroscopic length, lattice-parameter and microstructural changes in neutron-irradiated aluminum nitride due to annealing, J. Nucl. Mater. 191 (1992) 635-639.

[13]   C.S. Kim, T. Iseki, T. Yano, M. Tezuka, Mechanical-properties of neutron-irradiated AlN, J. At. Energy Soc. Jpn. 34 (1992) 335-341.

[14]   T. Yano, K. Ichikawa, M. Akiyoshi, Y. Tachi, Neutron irradiation damage in aluminum oxide and nitride ceramics up to a fluence of 4.2 x 10(26) n/m(2), J. Nucl. Mater. 283 (2000) 947-951.

[15]   T. Yano, T. Iseki, Swelling and microstructure of AlN irradiated in a fast-reactor, J. Nucl. Mater. 203 (1993) 249-254.

[16]   T. Yano, T. Iseki, Thermal and mechanical-properties of neutron-irradiated aluminum nitride, J. Nucl. Mater. 179 (1991) 387-390.

[17]   M. Akiyoshi, I. Takagi, T. Yano, N. Akasaka, Y. Tachi, Thermal conductivity of ceramics during irradiation, Fusion Eng. Des. 81 (2006) 321-325.

[18]   J.C. Nappé, Ph. Grosseau, F. Audubert, B. Guilhot, M. Beauvy, M. Benabdesselam, I. Monnet, Damages induced by heavy ions in titanium silicon carbide: Effects of nuclear and electronic interactions at room temperature, J. Nucl. Mater. 385 (2009) 304-307.

[19]   J.F. Ziegler, <http://www.srim.org/>.

[20]   F. Porte, J.P. Lecompte, J. Jarrige, A. Collange, P. Grosseau, B. Guilhot, Thermoluminescence of aluminium nitride: Influence of the thermal treatment, J. Eur. Ceram. Soc. 17 (1997) 1797-1802.

11

[21]   M. Benabdesselam, P. Iacconi, D. Lapraz, Ph. Grosseau, B. Guilhot, Thermoluminescence of AlN. Influence of synthesis processes, J. Phys. Chem. 99 (1995) 10319-10323.

[22]   J. Rosa, I. Tale, Mechanism of thermoluminescence in Al:O, Czech. J. Phys. 29 (1979) 810-824.

[23]   L. Trinkler, P. Christensen, N.A. Larsen, B. Berzina, Thermoluminescence properties of AlN ceramics, Radiat. Meas. 29 (1998) 341-348.

[24]   A.L. Martin, C.M. Spalding, V.I. Dimitrova, P.G. Van Patten, M.L. Caldwell, M.E. Kordesch, H.H. Richardson, Visible emission from amorphous AlN thin-film phosphors with Cu, Mn, or Cr, J. Vac. Sci. Technol. A: Vac Surf. Films 19 (2001) 1894-1897.

[25]   M.A.F.M. da Silva, R.B. Barthem, L.P. Sosman, Investigation of luminescence and optical absorption of K2LiAlF6:Cr3+ single crystals, J. Solid State Chem. 179 (2006) 3718-3723.

[26]   I. Sokólska, S. Kück, Optical characterization of Cr3+ doped LiTaO3 crystals relevant for laser application, Spectrochim. Acta Part A: Mol. Biomol. Spectrosc. 54 (1998) 1695-1700.

[27]   G.M. Salley, S.A. Basun, A.A. Kaplyanskii, R.S. Meltzer, K. Polgar, U. Happek, Chromium centers in stoichiometric LiNbO3, J. Lumin. 87-89 (2000) 1133-1135.

[28]   M.G. Brik, Crystal field analysis, electron-phonon coupling and spectral band shape Modeling in MgO:Cr3+, Z. Naturforsch. A: J. Phys. Sci. 60 (2005) 437-443.

[29]   M.G. Brik, V.A. Lebedev, E.V. Stroganova, Spectroscopic and crystal field studies of (Ce,Gd)Sc3 (BO3)4:Cr3+ crystals, J. Phys. Chem. Solids 68 (2007) 1796-1804.

[30]   A.R. Moon, M.R. Phillips, Defect clustering and color in Fe,Ti: [alpha]-Al2O3, J. Am. Ceram. Soc. 77 (1994) 356-367.

[31]   K. Kawabe, R.H. Tredgold, Y. Inuishi, Electrical and optical properties of AlN - a thermostable semiconductor, Electr. Eng. Jpn. 87 (1967) 62-70.

[32]   G.A. Cox, D.O. Cummins, K. Kawabe, R.H. Tredgold, On the preparation, optical properties and electrical behaviour of aluminium nitride, J. Phys. Chem. Solids 28 (1967) 543-548.

[33]   T.L. Tansley, R.J. Egan, Point-defect energies in the nitrides of aluminum, gallium, and indium, Phys. Rev. B 45 (1992) 10942.

[34]   T. Mattila, R.M. Nieminen, Ab initio study of oxygen point defects in GaAs, GaN, and AlN, Phys. Rev. B 54 (1996) 16676-16682.

[35]   M. Bickermann, B.M. Epelbaum, A. Winnacker, Characterization of bulk AlN with low oxygen content, J. Cryst. Growth 269 (2004) 432-442.

[36]   B.D. Evans, G.J. Pogatshnik, Y. Chen, Optical properties of lattice defects in [alpha]-Al2O3, Nucl. Instrum. Methods Phys. Res. Sect. B: Beam Interact. Mater. Atoms 91 (1994) 258-262.

[37]   T.J. Turner, J.H. Crawford, V centers in single crystal Al2O3, Solid State Commun. 17 (1975) 167-169.

[38]   D. Lapraz, Ph. Iacconi, D. Daviller, B. Guilhot, Thermostimulated luminescence and fluorescence of [alpha]-Al2O3:Cr3+ samples (Ruby): influence of the Cr3+ concentration, Phys. Status Solidi (a) 126 (1991) 521-531.

[39]   M. Beauvy, C. Dalmasso, C. Thiriet-Dodane, D. Simeone, D. Gosset, Damages in ceramics for nuclear waste transmutation by irradiation with swift heavy ions, Nucl. Instrum. Methods Phys. Res. Sect. B: Beam Interact. Mater. Atoms 242 (2006) 557-561.

[40]   J. Pasternak, L. Roskovcova, Optical absorption end of AlN single crystals, Phys. Status Solidi 26 (1968) 591.

[41]   G.A. Slack, L.J. Schowalter, D. Morelli, J.A. Freitas, Some effects of oxygen impurities on AlN and GaN, J. Cryst. Growth 246 (2002) 287-298.

[42]   M.J. Springis, J.A. Valbis, Visible luminescence of colour centres in sapphire, Phys. Status Solidi (b) 123 (1984) 335-343.

[43]   M. Toulemonde, C. Dufour, E. Paumier, Transient thermal-process after a high-energy heavy-ion irradiation of amorphous metals and semiconductors, Phys. Rev. B 46 (1992) 14362-14369.

[44]   M. Toulemonde, E. Paumier, C. Dufour, Thermal spike model in the electronic stopping power regime, Radiat. Eff. Defects Solids 126 (1993) 201-206.

[45]   A. Benyagoub, A. Audren, L. Thome, F. Garrido, Athermal crystallization induced by electronic excitations in ion-irradiated silicon carbide, Appl. Phys. Lett. 89 (2006) 241914.